Title
SOME RECENT PROGRESS IN STEEP FRONT CALCULA-TIONS FOR POROUS FLOW

Authors
Concus, P.
Kostlan, E.
Sethian, J.A.

Publication Date
1984

Lawrence Berkeley Laboratory
UNIVERSITY OF CALIFORNIA

Physics Division

Mathematics Department

Presented at the Sixth International Conference on Computing Methods in Applied Sciences and Engineering, Versailles, France, December 12-16, 1983

SOME RECENT PROGRESS IN STEEP FRONT CALCULATIONS FOR POROUS FLOW

P. Concus, E. Kostlan, and J.A. Sethian

January 1984

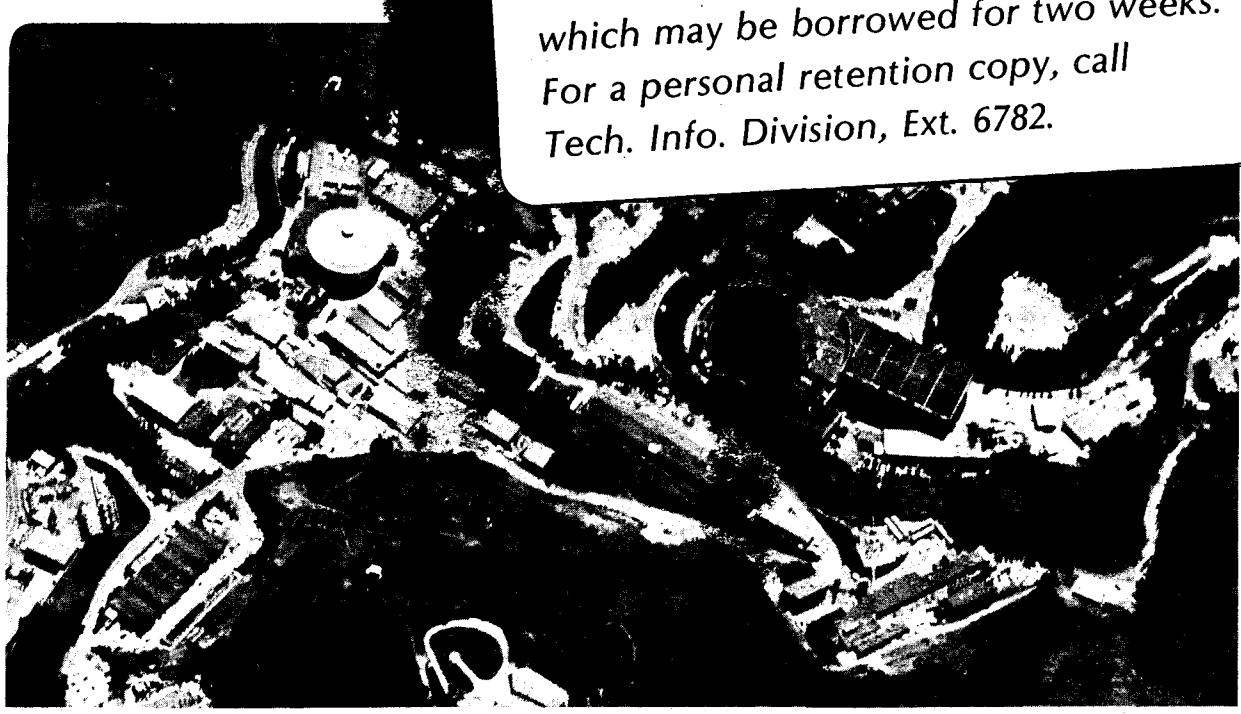

Prepared for the U.S. Department of Energy under Contract DE-AC03-76SF00098

DISCLAIMER

LBL-17221

SOME RECENT PROGRESS IN STEEP FRONT CALCULATIONS FOR POROUS FLOW

P. Concus, E. Kostlan, and J.A. Sethian

Lawrence Berkeley Laboratory
and
Department of Mathematics
University of California
Berkeley, California, 94720

January 1984

This work was supported in part by the Director, Office of Energy Research, Office of Basic Energy Sciences, Engineering, Mathematical, and Geosciences Division of the U.S. Department of Energy under Contract DE-AC03-76SF00098 and by the International Business Machines Corporation, Palo Alto Scientific Center, Palo Alto, CA.

SOME RECENT PROGRESS IN STEEP FRONT CALCULATIONS FOR POROUS FLOW

P. Concus, E. Kostlan, and J.A. Sethian

Lawrence Berkeley Laboratory
and
Department of Mathematics
University of California
Berkeley, California 94720
U.S.A.

A modification to the random choice method is investigated for solving the equations for multidimensional immiscible displacement in a porous medium. The principal feature of the modification is to represent multidimensional flow correctly by incorporating local properties of the flow into the one-dimensional Riemann solvers of the split random choice method. Advancing fronts are kept accurate and sharp. We perform a numerical experiment using the method to study the stabilizing effect of a small amount of physical capillary pressure on a case for which the advancing front is unstable.

INTRODUCTION

A central problem in petroleum reservoir simulation is to model the displacement of one fluid by another within a porous medium. Such problems may be characterized by the injection of a wetting fluid (e.g. water) into the reservoir at one or more points, displacing the non-wetting fluid (e.g. oil), which is being withdrawn at one or more recovery points. The nature of the front between the non-wetting fluid and the wetting fluid is of primary importance; one would like to withdraw as much oil as possible before water reaches the recovery points. A particularly troublesome phenomenon associated with the above procedure is fingering, in which small channels of water push through towards the recovery points, leaving oil behind.

In the design of numerical techniques to model petroleum reservoir flow, one is faced with the problem that the solution to the equations describing the fluid saturation within the reservoir can develop sharp fronts or discontinuities. Finite difference approximations to these equations smear out the front and may distort the nature of the interface, unless expensive mesh refinement is used. One can instead attempt to track the front between the two fluids; however, such techniques usually contain an intrinsic smoothing and thus can predict a stable interface in regimes where fingering should occur. One alternative to the above techniques, which serves as a foundation for the work presented here, is the random choice method, in which the generation of the solution at each time step is based on the exact solution of a collection of local Riemann problems.

In this paper, we apply a recently developed generalized version of the one-dimensional random choice method to two-dimensional reservoir simulation. In this improved technique, while the multi-dimensional solution is obtained through a sequence of one-dimensional problems, information about the two-dimensional solution is used to ensure that each of the one-dimensional problems correctly interprets the nature of the propagating fronts. The algorithm was first used in [5] to study the nature of fingering instability in the absence of capillary

pressure. It was applied subsequently to a five-spot waterflood for the case of a stable interface, also without capillary pressure [12].

We apply the technique here to a two-dimensional five spot waterflood problem for the case of an unstable interface and permit the inclusion of capillary pressure. Our numerical results indicate that the advancing front is kept sharp, and that the method is sufficiently free of artificial numerical stabilization so that the effects of including a small amount of capillary pressure can be observed numerically. We repeat here without change much of the material presented in [12], but include in greater detail a discussion of the modifications to the random choice method.

EQUATIONS OF MOTION

We consider the equations

$$\frac{\partial s}{\partial t} + \mathbf{q}\cdot\nabla[f(s)] - \epsilon\nabla\cdot[h(s)\nabla s] = 0 \tag{1}$$

$$\nabla\cdot\mathbf{q} = 0 \tag{2}$$

$$\mathbf{q} = -\lambda(s)\nabla p\ , \tag{3}$$

which in nondimensional form (see [2]) are, respectively, the Buckley-Leverett equation, incompressibility relation, and Darcy's Law. These equations describe the flow of two immiscible, incompressible fluids through a homogeneous porous medium in the absence of gravitational effects (see [10,11]). The quantity $s = s(x,y,t)$ is the saturation (the fraction of available volume at the point (x,y) and time t filled with wetting fluid, e.g. water), $\mathbf{q} = \mathbf{q}(x,y,t)$ is the total velocity of the fluid, and $p = p(x,y,t)$ is the global pressure [3]. The quantities $f(s)$, $h(s)$, and $\lambda(s)$ are functions of the relative permeabilities and capillary pressure, which are empirically determined functions of saturation, and of the viscosities (which are assumed constant). The parameter $\epsilon \geq 0$, which we shall take to be small, measures the relative magnitude of the diffusive (capillary pressure) forces. For immiscible fluids, we take the total mobility $\lambda(s)$ to be represented by

$$\lambda(s) = s^2 + (1-s)^2/\mu\ , \tag{4}$$

where μ is the ratio of the viscosity of the non-wetting fluid to that of the wetting fluid. The corresponding fractional flow function $f(s)$ is

$$f(s) = s^2/\lambda(s)\ , \tag{5}$$

and we take $h(s) = \frac{2}{\mu}(1-s)^3 f(s)$.

Equations (2) and (3) together form an elliptic equation. For our problems of interest, (1) is hyperbolic ($\epsilon = 0$) or nearly hyperbolic ($\epsilon \ll 1$) and as such can develop discontinuities or steep fronts in s, even for arbitrarily smooth initial data. To analyze the nature of the discontinuities, we consider (1) in one space dimension $\epsilon = 0$, namely,

$$s_t + (f(s))_x = s_t + f'(s)s_x = 0\ . \tag{6}$$

Here, we have taken the velocity as unity for simplicity.

Suppose for a given problem the fractional flow function satisfies $f_{ss} > 0$ and thus f is concave up. It can easily be shown that the characteristics for (6) are straight lines leaving the x-axis with slope

$$\frac{dx}{dt} = f'(s) . \tag{7}$$

Since $f_{ss} > 0$, then $f'(s)$ is an increasing function of s. Consider the initial data

$$s(x,0) = \begin{cases} s_l , & x < 0 \\ s_r , & x > 0 , \end{cases} \tag{8}$$

where s_l and s_r are constants. If $s_l < s_r$, then $f'(s_l) < f'(s_r)$ and information from the left is propagating slower than information from the right. The entropy condition, which requires that all characteristics reach back to the initial data, thus dictates that a rarefaction wave will form between the two (see Fig. 1). Conversely, if $s_l > s_r$, then $f'(s_l) > f'(s_r)$, and information from the left propagates faster than information from the right; the entropy condition thus dictates the formation of a shock propagating with speed $\dfrac{f(s_r) - f(s_l)}{s_r - s_l}$ (Fig. 2).

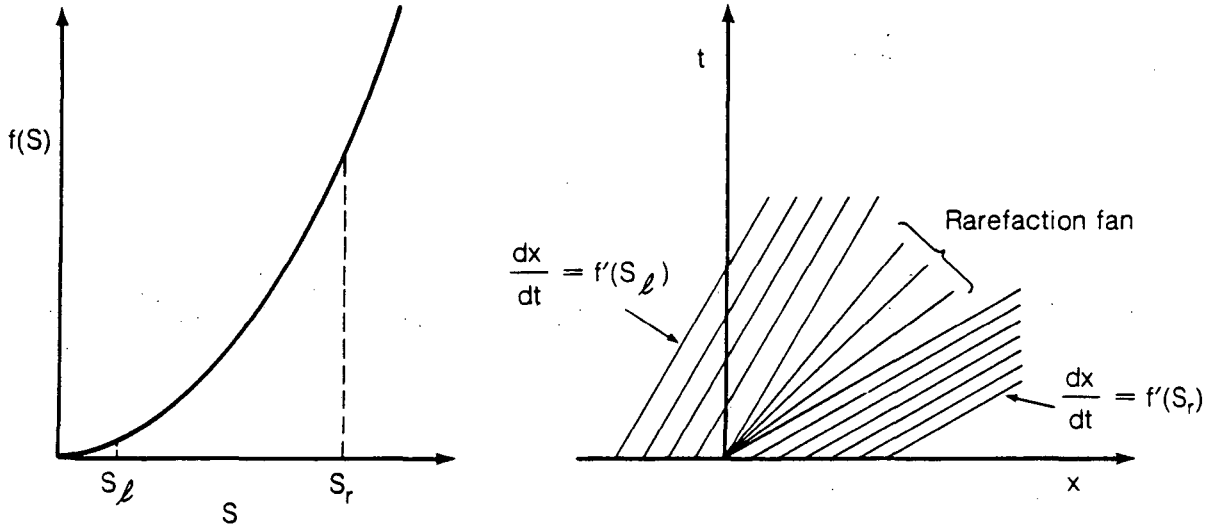

Figure 1
Riemann problem solution, convex $f(s)$, $s_l < s_r$.

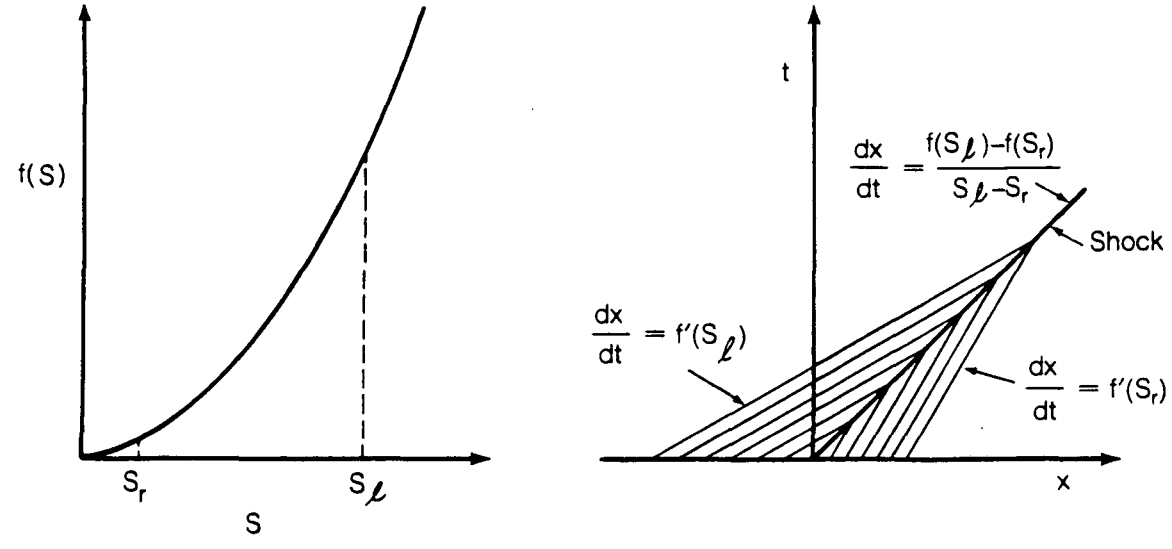

Figure 2
Riemann problem solution, convex $f(s)$, $s_l > s_r$.

In the case of more general f, one has the generalized entropy condition (Oleinik's condition E), which determines the type of admissible shocks: Given s_- and s_+, where s_- and s_+ are the limiting values to the left and the right of a discontinuity, respectively, a solution to (6) exists, is unique, and depends continuously on the initial data if the following holds

$$1) \quad \text{if } s_- < s_+ \text{ then } \frac{f(s_+) - f(s_-)}{s_+ - s_-} \leq \frac{f(s_+) - f(s)}{s_+ - s}$$

$$\text{for all } s \in [s_-, s_+].$$

$$2) \quad \text{if } s_+ < s_- \text{ then } \frac{f(s_+) - f(s_-)}{s_+ - s_-} \geq \frac{f(s_+) - f(s)}{s_+ - s}$$

$$\text{for all } s \in [s_+, s_-].$$

Geometrically, this condition translates into the statement that admissible shocks are those such that (1) if $s_- < s_+$, then the chord connecting $(s_-, f(s_-))$ and $(s_+, f(s_+))$ must lie below f, (2) if $s_+ < s_-$, then the chord connecting $(s_+, f(s_+))$ and $(s_-, f(s_-))$ must lie above f. In the case of a purely convex f, the above produces the situations described earlier; in particular, a shock cannot be allowed to connect the left state with the right state in Fig. 1. For non-convex f, the above condition also rules out such waves as shocks which move faster or slower than the characteristics on both of their sides.

In our problem, the fractional flow function (5) contains one inflection point (see Fig. 3). Thus the wave connecting the left and right states will be either a shock, rarefaction, or combination of the two. We determine the appropriate wave as follows. Given s_l and s_r, the left and right states respectively,

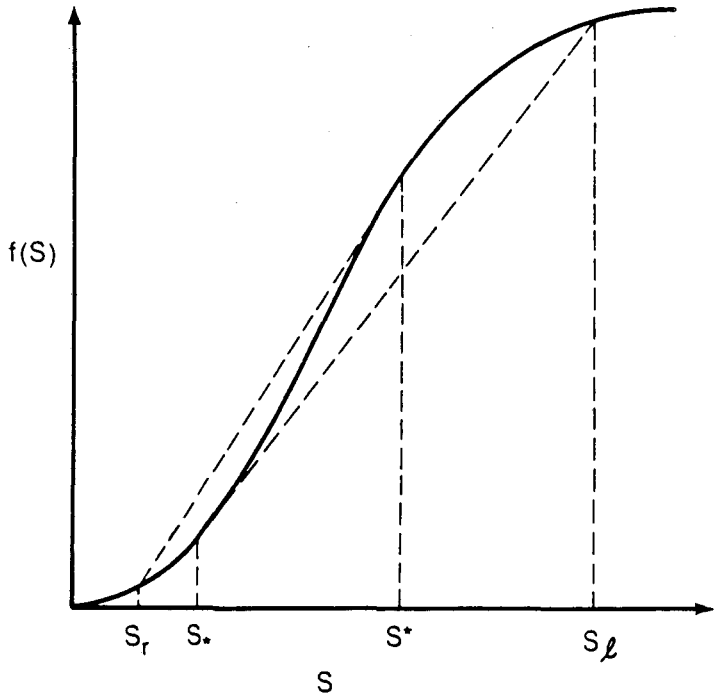

Figure 3
Fractional flow function with convex and concave hulls
for compound wave solution, $s_l > s_r$.

1) If the chord connecting $(s_l, f(s_l))$ and $(s_r, f(s_r))$ does not intersect f, then the curve is convex up or down between the two points. If $f'(s_l) > f'(s_r)$, then by the generalized entropy condition a shock must connect s_l with s_r; if $f'(s_l) < f'(s_r)$, then a rarefaction connects the two states.

2) Suppose the chord connecting the left and right states intersects f. Then there exists a point s^* between s_r and s_l such that the chord from $(s_r, f(s_r))$ to $(s^*, f(s^*))$ is tangent to f at $(s^*, f(s^*))$ (the case $s_r < s_l$ is shown in Figs. 3, 4). The wave connecting s_r to s^* is a shock and the wave connecting s^* to s_l is a rarefaction.

The above choices apply to the case in which the advection speed q is unity. If q is positive, but not 1, the wave speeds are merely scaled by q. If q is negative, the roles of s_l and s_r are interchanged in the above arguments.

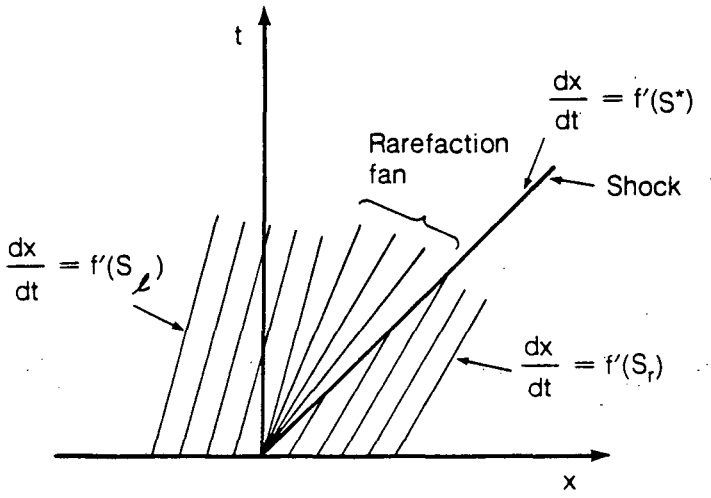

Figure 4
Riemann problem solution, compound wave, $s_l > s_r$.

NUMERICAL ALGORITHM

We consider as an example the standard diagonal geometry quarter five spot problem. That is, we assume a square domain D, centered at (½,½), with sides of unit length, and (1)-(3) holding inside the domain. At (0,0) we place a source of unit strength; at (1,1) we place a sink of unit strength. We have the initial conditions

$$s(x,y,0) = 0 \quad \text{for} \quad (x,y) \neq (0,0)\,, \tag{9}$$

together with the boundary conditions

$$s(0,0,t) = 1 \tag{10}$$

$$\frac{\partial s}{\partial \nu} = \frac{\partial p}{\partial \nu} = 0 \ \text{ on the edges of the square}\,, \tag{11}$$

where ν is the normal to the boundary. The above problem may be summarized by saying that we inject wetting fluid ($s = 1$, water) into the lower left corner with strength so that the flux is equal to unity, and withdraw non-wetting fluid ($s = 0$, oil) from the upper right corner at the same rate; at no other points can fluid enter or leave the domain.

The numerical algorithm used to solve the equations of motion is based on a generalized random choice method for the hyperbolic or nearly hyperbolic equation (1) coupled to a successive over-relaxation method for the elliptic equation (2),(3). The random choice method is a numerical technique developed in [4] and is based on a constructive existence proof introduced in [9]. We briefly describe the technique below.

Consider the equation

$$s_t + u[f(s)]_x = 0 . \tag{12}$$

Place a uniformly spaced grid of mesh length h along the x axis and let s_i^n be the value $s(ih, n\Delta t)$; thus we view s as a piecewise constant function, constant within each interval $[(i-\frac{1}{2})h, (i+\frac{1}{2})h]$. This produces a collection of initial value Riemann problems of the form

$$s = \begin{cases} s_l , & x < (i+\frac{1}{2})h \\ s_r , & x > (i+\frac{1}{2})h , \end{cases} \tag{13}$$

where $s_l = s_i^n$ and $s_r = s_{i+1}^n$. The solution is then updated in time by solving each Riemann problem exactly, with the type of wave used to connect the two states (shock, rarefaction, compound) determined as discussed above. The solution is then sampled to produce new values of s; we use a sampling based on a van der Corput sequence, see [4]. The time step Δt is chosen to be the largest possible value such that the separate Riemann problems do not interact; that is,

$$\Delta t \, |q| \max_i f'(s_i^n) \leq h . \tag{14}$$

This technique was first applied to porous flow problems in [5].

A natural way to extend the above one-dimensional technique to two dimensions is to split the two-dimensional hyperbolic equation ($\epsilon = 0$)

$$s_t + \mathbf{q} \cdot \nabla [f(s)] = 0 \tag{15}$$

into two steps; first a one-dimensional problem in the x direction

$$s_t + u \frac{\partial}{\partial x}(f(s)) = 0 \tag{16}$$

is solved, followed by a one-dimensional problem in the y direction

$$s_t + v \frac{\partial}{\partial y}(f(s)) = 0 , \tag{17}$$

where $\mathbf{q} = (u, v)$. Unfortunately, a front not parallel to either the x or y axis can be misinterpreted during one of the sweeps, as may be seen by considering the following example. Suppose the interface between water and oil is lying diagonal to the grid, and the velocity vector at a point on the front is as shown in Fig. 5. It is clear that water is displacing oil, however if

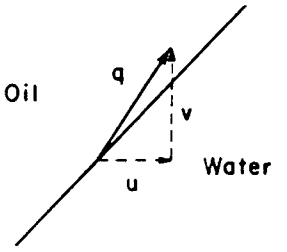

Figure 5
Obliquely propagating discontinuity front.

one looks simply at the component of the velocity vector in the x direction, oil seems to be displacing water and hence the solution to the one-dimensional problem will not accurately portray what is happening. Errors due to the above phenomenon can be significant; examples of their effect may be found in [8]. The technique we use, introduced in [5], first determines the correct orientation by analyzing the two-dimensional situation, and uses this information in each of the one-dimensional sweeps.

The details of the modified Riemann problem solutions are illustrated in Figs. 6-8. For the purely convex case, the modified (entropy violating) solutions corresponding to Figs. 1 and 2 are depicted in Figs. 6 and 7, respectively. Note that the configuration of the rarefaction shown in Fig. 7 depends on the time Δt at which the solution is to be sampled. The modified solution corresponding to the compound wave with $s_r < s_l$ for the porous flow $f(s)$ (Fig. 3) is shown in Fig. 8; the concave hull in Fig. 3, rather than the convex hull, is used in its construction. The compound wave for $s_l < s_r$ is constructed analogously. Further discussion of the algorithm can be found in [5].

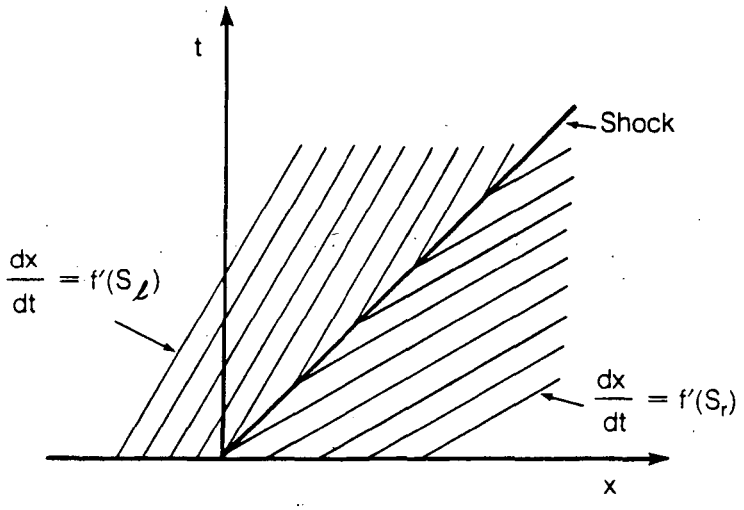

Figure 6
Modified Riemann problem solution, convex $f(s)$, $s_l < s_r$.

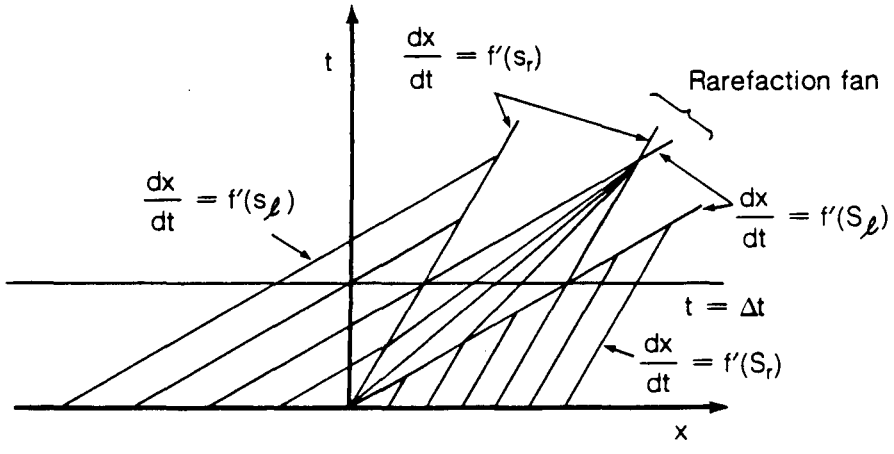

Figure 7
Modified Riemann problem solution, convex $f(s)$, $s_l > s_r$.

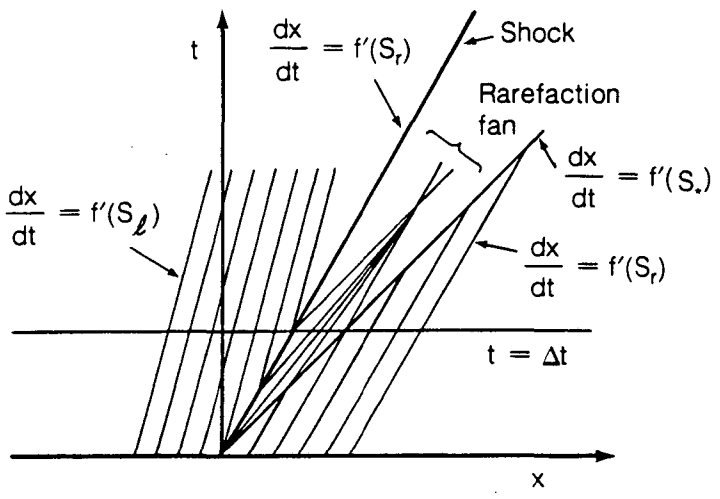

Figure 8
Modified Riemann problem solution, compound wave, $s_l > s_r$.

We now describe the algorithm for solving Equations (1)-(3). With time step Δt, let $s_{i,j}^n$ be the value of the saturation at $s(ih, jh, n\Delta t)$; here we assume that $s_{i,j}^n$ is defined on a square grid i, j of mesh length h imposed on the domain. The pressures $p_{i,j}^n$ are taken at the same grid points, and the velocities $u_{i+\frac{1}{2},j}$, $v_{i,j+\frac{1}{2}}$ are to be evaluated at the midpoints of the sides of a cell (see Fig. 9). Assuming $s_{i,j}^n$ is known, we now describe the algorithm used to obtain $s_{i,j}^{n+1}$ from $s_{i,j}^n$.

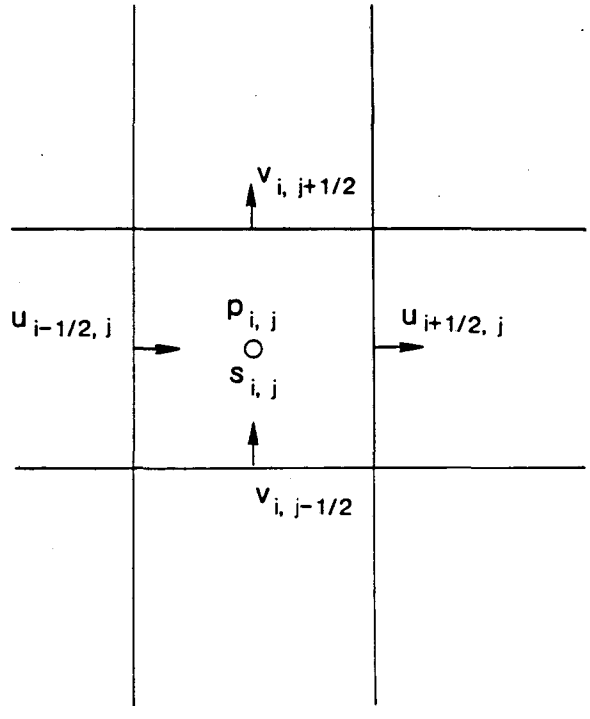

Figure 9
Staggered grid for p, s, and $\mathbf{q}$.

The first step is to calculate $p^n_{i,j}$ from $s^n_{i,j}$. Substituting (3) into (2) yields the elliptic equation for p

$$\nabla\cdot(-\lambda(s)\nabla p) = 0\,. \tag{18}$$

Corresponding to differencing a typical component of (3) as

$$u_{i+\frac{1}{2},j} \approx \frac{(\lambda(s_{i+1,j})+\lambda(s_{i,j}))\,(p_{i+1,j}-p_{i,j})}{2h}\,, \tag{19}$$

we approximate (18) with a centered difference scheme, which at a general interior point is

$$\begin{aligned}
&-\frac{(\lambda(s_{i+1,j})+\lambda(s_{i,j}))(p_{i+1,j}-p_{i,j})}{2h^2}\\
&+\frac{(\lambda(s_{i,j})+\lambda(s_{i-1,j}))(p_{i,j}-p_{i-1,j})}{2h^2}\\
&-\frac{(\lambda(s_{i,j+1})+\lambda(s_{i,j}))(p_{i,j+1}-p_{i,j})}{2h^2}\\
&+\frac{(\lambda(s_{i,j})+\lambda(s_{i,j-1}))(p_{i,j}-p_{i,j-1})}{2h^2} \approx 0\,.
\end{aligned} \tag{20}$$

This scheme conserves the flux $-\lambda(s)\nabla p$ through each cell, and consequently ensures that there are no fictitious sources or sinks introduced by the finite difference approximation into the calculation.

Along the four sides, the discrete form of the boundary conditions (11) is used to modify (20). At the edges of the injection and production cells the flux is taken to be ¼, appropriately directed. From the pressures, which are obtained by solving the resulting linear system, the velocity components are calculated using (19) and its counterparts.

With u^n , v^n, p^n, and s^n known, we now solve (1) to determine s^{n+1} at the grid points. We first determine whether the two-dimensional advection velocity $\mathbf{q} = (u,v)$ causes water to displace oil or oil to displace water; this can easily be accomplished by checking the angle between $\mathbf{q}$ and ∇f. Then, we determine if the two one-dimensional sweeps for the advective term

$$s_t + u\frac{\partial}{\partial x}(f(s)) = 0 \tag{21}$$

$$s_t + v\frac{\partial}{\partial y}(f(s)) = 0 \tag{22}$$

both interpret the situation in the same way as does the two-dimensional analysis. For example, if water is displacing oil, we check to see that the situation holds for both of the one-dimensional sweeps. If so, we may simply solve (21) and then (22) using the random choice method described earlier to obtain a new value $\tilde{s}^n$ of s. Suppose, however, that one of the sweeps indicates an orientation different from the actual one described by the two-dimensional analysis, such as in Fig. 5, where, although water is clearly displacing oil, the x sweep indicates oil displacing water. In order to force the wave connecting the two states to be of the same type as that determined by the two-dimensional analysis, we switch the role of convex and concave hulls in our Riemann solution (this can be accomplished by interchanging s_l and s_r in the Riemann solver). Although the one-dimensional solution constructed may violate the generalized entropy condition (e.g. we now allow rarefaction shocks), the proper two-dimensional information is represented in each of the one-dimensional problems, and the generation of shocks and rarefaction waves due purely to grid orientation has been avoided.

To obtain the value of s^{n+1} from $\bar{s}^n$, one finally carries out a sweep

$$s_t - \epsilon \nabla \cdot [h(s) \nabla s] = 0$$

for the contribution of the diffusive capillary-pressure term. Since ϵ is small, we take for our numerical experiments simply an explicit forward step

$$s^{n+1} = \bar{s}^n + \epsilon \Delta t \{\nabla \cdot [h(s) \nabla s]\}_{s=\bar{s}^n},$$

using the spatial discretization represented in (20).

RESULTS

Numerical results are presented for the standard diagonal geometry quarter five-spot test problem discussed in the previous section for waterflood of a petroleum reservoir. A 40×40 spatial grid is placed on the unit square, and the viscosity ratio for the first test problem is taken to have the value $\mu = 5$. For this value of μ, the mobility ratio M at the front is approximately 1.18, which is slightly greater than the critical value $M = 1$. Hence according to the linearized theory and the numerical results in [5], the advancing front should be unstable in the absence of capillary pressure, i.e. for $\epsilon = 0$.

Figure 10 shows the computational results for $\epsilon = 0$. Contours are drawn in saturation increments of 0.1 at three successive time values. Because the contour plotting package displaces contours that should lie on top of one another, the advancing front is shown as a band of adjacent contour lines, rather than as the sharp front produced by the numerical calculations. Observe that unstable "fingering" of the front develops spontaneously during the calculation. (The smaller undulations, which are of the order of a mesh spacing and are stable, are inherent in the random choice method and the interpolations introduced by the contour plotting program.)

Figure 11 shows the effect of including a small amount of capillary pressure ($\epsilon = 0.01$). The fingering instability of Fig. 10 is not evident in this case.

For the second test problem the viscosity ratio is taken to have the value $\mu = 10$, corresponding to which the mobility ratio at the front is $M \approx 1.40$. Figures 12, 13, and 14 show the computational results for $\epsilon = 0$, $\epsilon = 0.01$, and $\epsilon = 0.05$, respectively. Here, the results are in accord with the expectation that the front should be more unstable than for the smaller mobility ratio of Figs. 10 and 11. The effects on the fingering instability of including successively larger amounts of capillary pressure can be seen.

These results indicate that the modified random choice method holds promise as a device for studying sharp fronts in a porous medium. It appears sufficiently free of artificial numerical stabilization of an unstable front, so that the physical effects of including small amounts of capillary pressure can be investigated computationally. Computational results for the five-spot problem in the stable regime are given in [12].

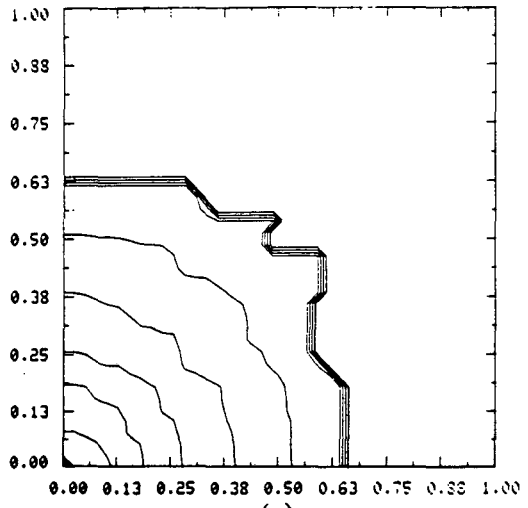

(a)

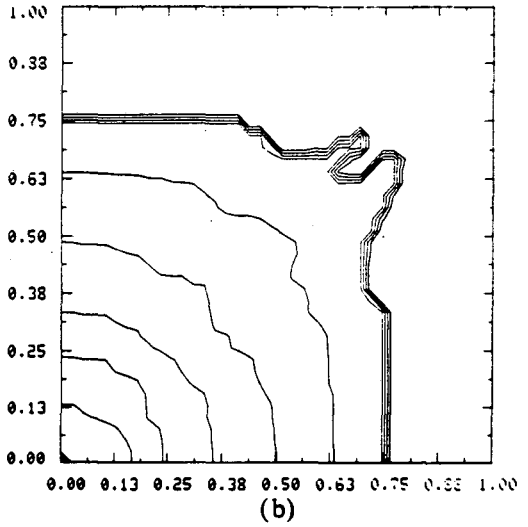

(b)

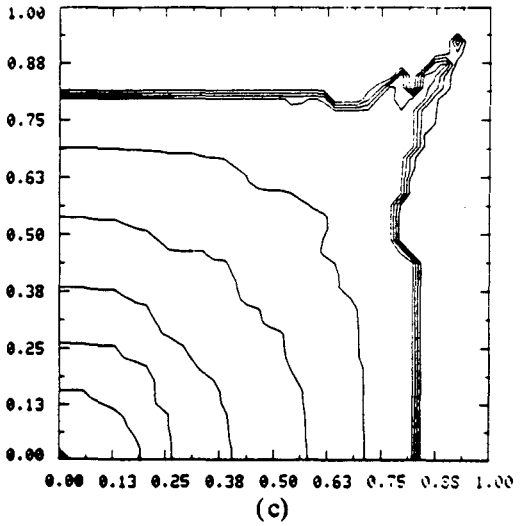

(c)

Figure 10
Saturation contours for $\mu = 5$, $\epsilon = 0$
at times t = (a) 0.80, (b) 1.20, (c) 1.50.

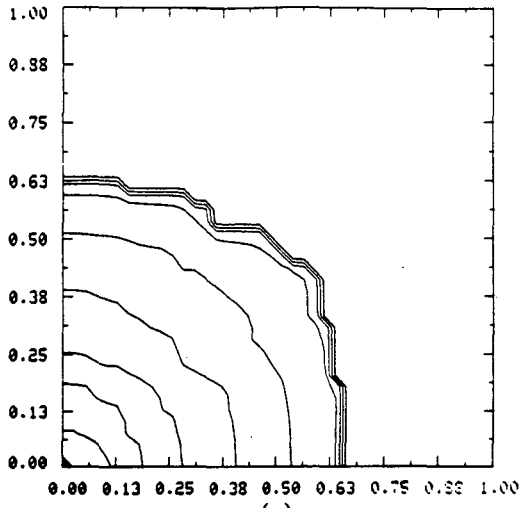

(a)

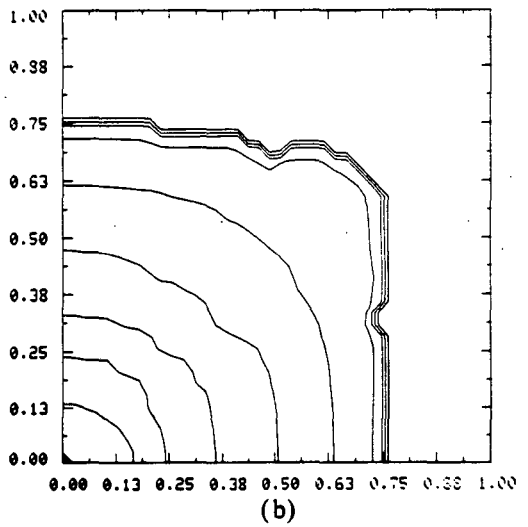

(b)

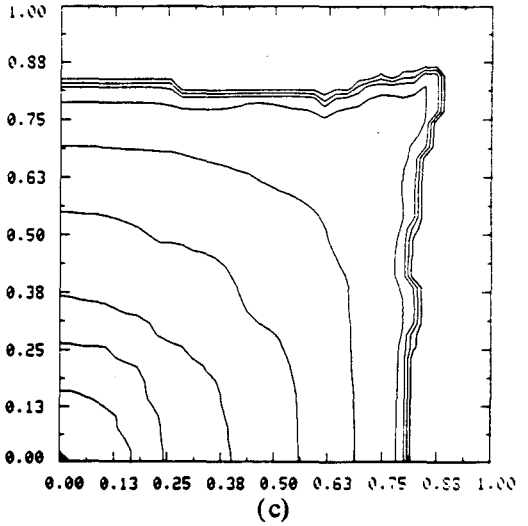

(c)

Figure 11
Saturation contours for $\mu = 5$, $\epsilon = 0.01$
at times t = (a) 0.79, (b) 1.20, (c) 1.50.

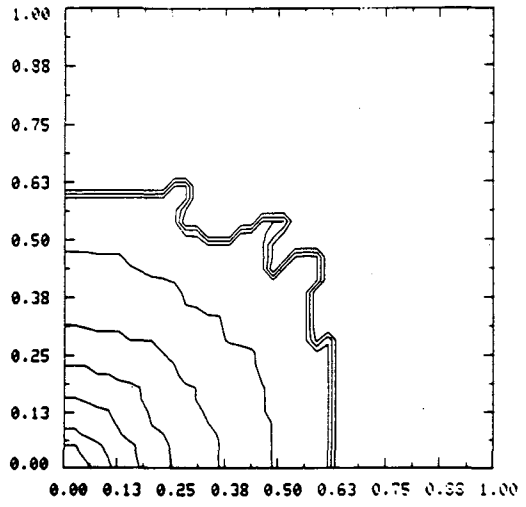

(a)

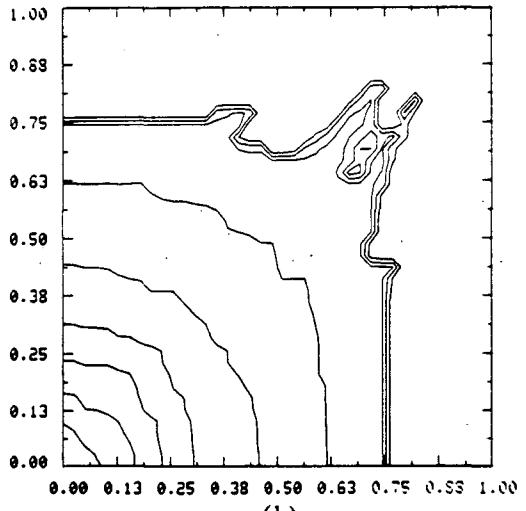

(b)

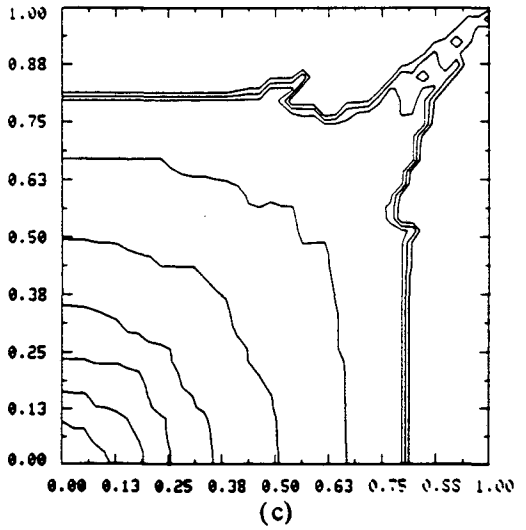

(c)

Figure 12
Saturation contours for $\mu = 10$, $\epsilon = 0$
at times $t =$ (a) 0.60, (b) 1.00, (c) 1.19.

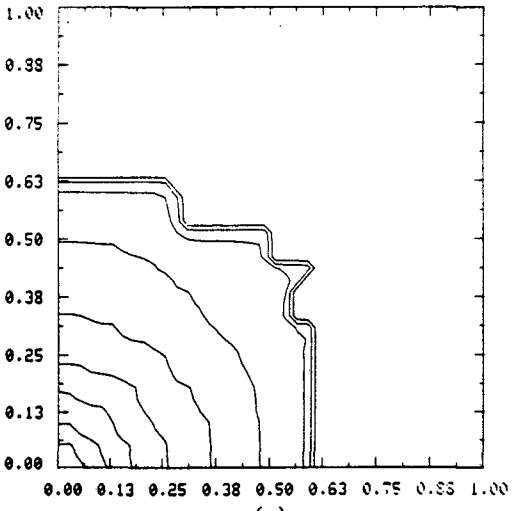

(a)

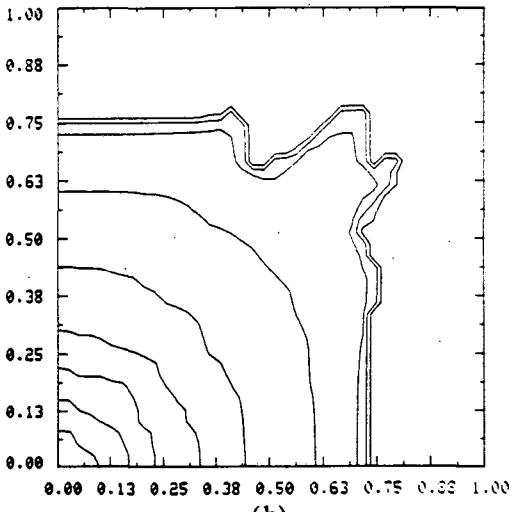

(b)

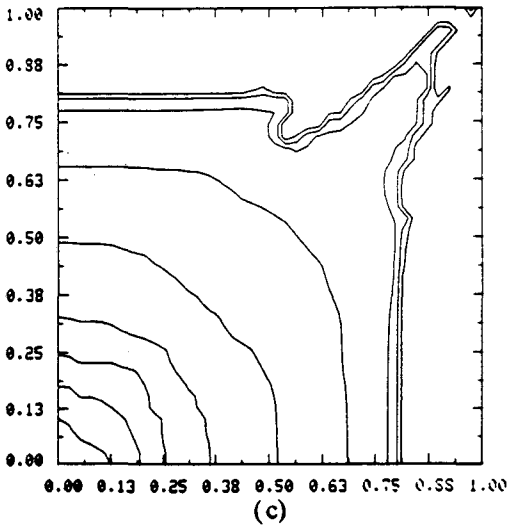

(c)

Figure 13
Saturation contours for $\mu = 10$, $\epsilon = 0.01$
at times $t =$ (a) 0.60, (b) 0.99, (c) 1.17.

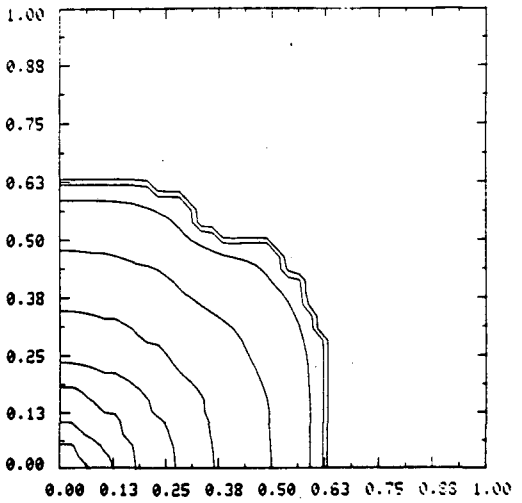

(a)

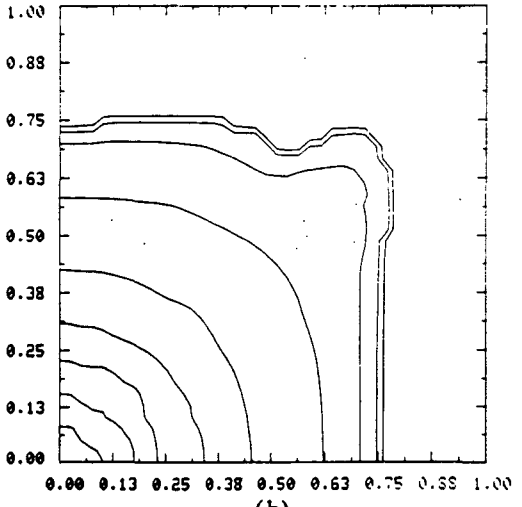

(b)

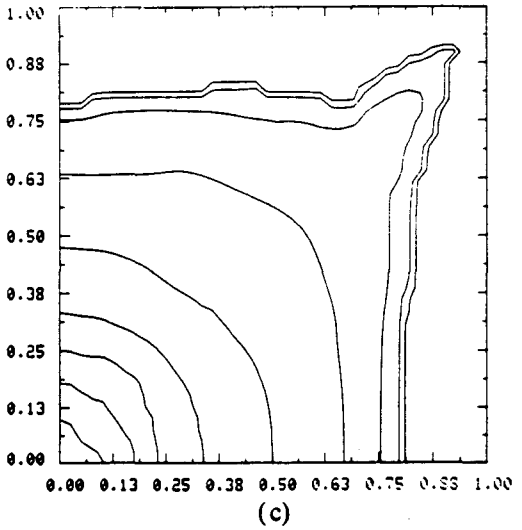

(c)

Figure 14
Saturation contours for $\mu = 10$, $\epsilon = 0.05$
at times $t =$ (a) 0.60, (b) 0.99, (c) 1.20.

ACKNOWLEDGMENTS

We are pleased to acknowledge Alexandre Chorin for helpful conversations concerning the modified random choice method. This work was supported in part by the Director, Office of Energy Research, Office of Basic Energy Sciences, Engineering, Mathematical, and Geosciences Division of the U.S. Department of Energy under Contract DE-AC03-76SF00098, and by the International Business Machines Corporation, Palo Alto Scientific Center, Palo Alto, CA.

REFERENCES

[1] Albright, N., Concus, P., and Proskurowski, W., Numerical solution of the multidimensional Buckley-Leverett equation by a sampling method, Paper SPE 7681, Soc. Petrol. Eng. Fifth Symp. on Reservoir Simulation, Denver, CO., Feb., 1979.

[2] Anderson, C. and Concus, P., A stochastic method for modeling fluid displacement in petroleum reservoirs, in Lecture Notes in Control and Information Sci., 28 (Springer-Verlag, Berlin-Heidelberg-New York, 1980), pp. 827-841.

[3] Chavent, G., A new formulation of diphasic incompressible flows in porous media, in Lecture Notes in Math., 503 (Springer-Verlag, Berlin-Heidelberg-New York, 1976), pp. 258-270.

[4] Chorin, A.J., Random choice solution of hyperbolic systems, J. Comput. Phys., 22 (1976) 517-533.

[5] Chorin, A.J., The instability of fronts in a porous medium, Comm. Math. Phys., 91 (1983) 103-116.

[6] Colella, P., Glimm's Method for Gas Dynamics, SIAM J. Sci. Statist. Comput., 3 (1982) 76-110.

[7] Concus, P. and Proskurowski, W., Numerical solution of a nonlinear hyperbolic equation by the random choice method, J. Comput. Phys., 30 (1979) 153-166.

[8] Crandall, M. and Majda, A., The method of fractional steps for conservation laws, Numer. Math., 34 (1980) 285-314.

[9] Glimm, J., Solution in the large for nonlinear hyperbolic systems of Equations, Comm. Pure Appl. Math., 18 (1965) 697-715.

[10] Peaceman, D.W., Fundamentals of Numerical Reservoir Simulation, (Elsevier, Amsterdam-Oxford-New York, 1977).

[11] Scheidegger, A.E., The Physics of Flow in Porous Media, (University of Toronto Press, Toronto, 1974).

[12] Sethian, J.A., Chorin, A.J., and Concus, P., Numerical solution of the Buckley-Leverett equations, Paper SPE 12254, Soc. Petrol. Eng. Seventh Symp. on Reservoir Simulation, San Francisco, CA, Nov. 1983.

TECHNICAL INFORMATION DEPARTMENT
LAWRENCE BERKELEY LABORATORY
UNIVERSITY OF CALIFORNIA
BERKELEY, CALIFORNIA 94720